Moderation of summertime heat-island phenomena via modification of the urban form in the Tokyo metropolitan area

Sachiho A. Adachi[1], Fujio Kimura[2], Hiroyuki Kusaka[2], Michael G. Duda[3], Yoshiki Yamagata[4], Hajime Seya[4,5], Kumiko Nakamichi[4,6], and Toshinori Aoyagi[7]

1 Advanced Institute for Computational Science, RIKEN,
7-1-26 Minatojima-minamimachi Cyuoku, Kobe, Japan, sachiho.adachi@riken.jp
2 Center for Computational Sciences, University of Tsukuba,1-1-1 Tennoudai, Tsukuba, Japan
3 National Center for Atmospheric Research, 3090 Center Green Drive, Boulder, Colorado, USA
4 National Institute for Environmental Studies, 16-2 Onogawa, Tsukuba, Japan
5 Hiroshima University, 1-3-2 Kagamiyama, Higashi-Hiroshima, Japan
6 Tokyo Institute of Technology, 2-12-1 Ookayama Meguro-ku, Tokyo, Japan
7 Meteorological Research Institute, 1-1 Nagamine, Tsukuba, Japan

dated : 15 Jun 2015

1. Introduction

Moderation of the urban heat island is expected to become part of an adaptation strategy to global climate change because urban heat-island mitigation should be mostly implemented by local governments (e.g. Adachi et al. 2012). Many methods have been proposed to mitigate urban heat-island effects, such as changes in the urban form, greening of parking lots and building walls, increasing roof albedo, and changes in pavement materials. This study focused on changes in urban form and investigated the moderation of nighttime surface air temperatures in the Tokyo metropolitan area (TMA) through simulations of dispersed- and compact-city scenarios at the current population level. This study has been published in Journal of Applied Meteorology and Climatology. Most of text and figures in the extended abstract are excerpts from Adachi et al. (2014).

2. Method

2.1 Experimental Design and Model

The numerical experiments listed in Table 1 were conducted to evaluate the effect of moderation of the urban form on the urban heat island. The simulation CTL_o was a control simulation for 2010 using the current urban situation. URB_d and URB_c were simulations to estimate the impact of changes in the urban form on urban climate. The estimation method of the dispersed-city and compact-city scenarios are described in section 2.2.

For these experiments, the Weather Research and Forecast model V3.1.1 (hereafter, WRF) (Skamarock et al., 2008) were used. The model domains are a nested system with three grids with horizontal spatial resolutions of 20 km, 4 km, and 2 km, respectively (Fig. 1). A total of 31 vertical model levels were used, and the height of the lowest level was set at approximately 30 m above ground level. The initial and boundary conditions for the WRF model were provided from the National Centers for Environmental Prediction (NCEP) and the National Center for Atmospheric Research (NCAR) reanalysis data (Kalnay et al., 1996). The simulation period was from 25 July to 1 September 2010, and the results for August were used for analysis. The other settings the physical scheme options are listed in Table 2.

Table 1. Experimental Design

Run name	Exp description	Boundary data	Land use	AH
CTL_o	Hindcast simulation	NCEP reanalysis data in 2010	Current urban situation (Original)	AH of current urban situation
URB_d	Impact of urban scenario		Dispersed-city scenario	AH of dispersed-city scenario
URB_c	Impact of urban scenario		Compact-city scenario	AH of compact-city scenario

Table 2. Physical scheme options used in the WRF model

Physical options	*Schemes*
Cloud microphysics	WSM 6-class graupel scheme
Convective parameterization	Kain–Fritsch (new Eta) scheme
Radiation scheme	RRTMG radiation scheme
Boundary layer	Mellor–Yamada–Janjic TKE scheme
Surface layer	Monin–Obukhov (Janjic) scheme
Land surface model	Noah land-surface model
Urban model	Single-layer urban canopy model

2.2 Urban Scenarios

This study assumed a current urban scenario and two other urban scenarios, the dispersed-city and compact-city scenarios, to estimate the moderation of the urban heat island by differences in urban form. The land-use data for the current urban scenario were classified into seven categories as follows: forest, cropland, paddy, grassland, bare, water area, and urban. Each land-use category was estimated by applying the improved subspace method (Bagan and Yamagata, 2010) using Landsat images and is presented as the fraction of data on a 1-km square mesh. The following sources of sensible and latent anthropogenic heat fluxes (AH) were considered for the current urban scenario: (1) the AH from residential and commercial buildings, (2) The AH from road transport. The total AH fluxes per 1-km mesh cell was obtained as the sum of AH from buildings and transport. The population data, provided by the national population census in 2005 and published by the Ministry of Internal Affairs and Communications (MIC), were used to determine the nighttime population density in the current urban scenario. The maps of urban fraction, daily mean AH, and population for the current urban scenario are shown in Figs. 2a, 2f, and 2k, respectively. The urban area was distributed along the railway. A larger AH was determined closer to the central area.

The dispersed-city and compact-city scenarios were produced using a spatially explicit land-use model (Yamagata et al. 2011). The model is a land-use equilibrium model entirely based on urban economic theory. The land-use model considers three different agents, namely households, developers, and absentee landlords, and determines the location of housing to maintain a balance between utility maximization for households and profit maximization by developers and absentee landlords. The details of this spatially explicit land-use model are described in Yamagata and Seya (2013) and Yamagata et al. (2013). To show the possible range of changes in the urban form in the TMA, the following conditions were assumed in the land-use model. The strategy for the dispersed-city scenario was automobile dependent and included (1) free purchase costs for a car, (2) no fuel cost for a car, and (3) toll-free expressways. Alternatively, the compact-city scenario assumed (1) a reduction in the land available for residential buildings in areas more than one kilometer away from train stations, and (2) the

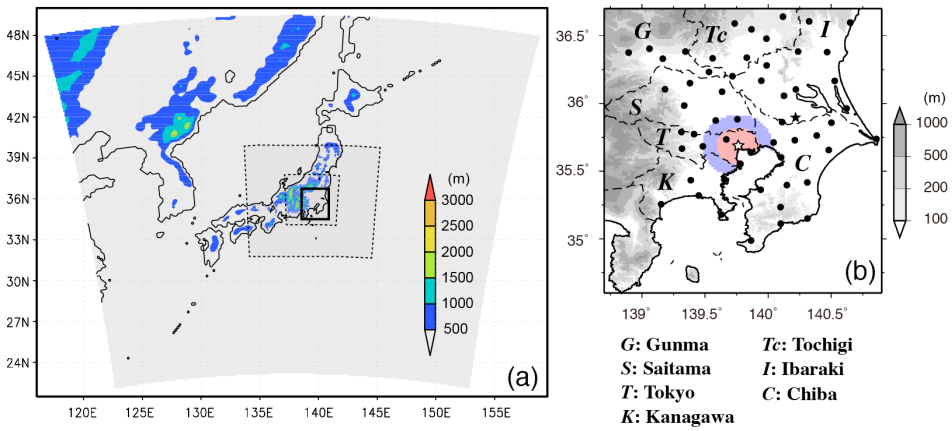

Fig. 1 (a) Simulation domains of the WRF model. The dotted squares indicate the second and third domains. (b) The analysis area, which is shown as a thick lined square in (a). Stars and black dots indicate the locations of AMeDAS observation stations. White and black stars indicate the locations of the Tokyo and Ryugasaki AMeDAS stations, respectively. The gray color indicates the topography. Red and blue colored areas are defined as Region i and Region ii, that are located within 15 km and 25 km away from Tokyo AMeDAS station, respectively. The other areas are defined as Region iii. (Fig.1 in Adachi et al. (2014) ©American Meteorological Society. Used with permission.)

prohibition of car use. The urban fractions in the dispersed- and compact-city scenarios were determined by the land-use model according to the above assumptions. The increased/decreased portion in the urban area was balanced by changing the most dominant land-use except for urban in a grid cell. The distributions of AH and population were estimated in accordance with the increase or decrease in households. The distributions of urban parameters in the two urban scenarios are illustrated in Fig. 2. The residential area expands to the suburbs, with a lower cost of commuting in the dispersed city (Figs. 2b and 2d). The AH also increases in suburban areas due to frequent car use and the expansion of residential areas. In contrast, the urban distribution in the compact city displays a similar pattern to the current urban situation (Fig. 2c), while the AH is enhanced in the central part of the TMA because of the concentration of people and the increase in floor area in that area (Figs. 2h and 2j).

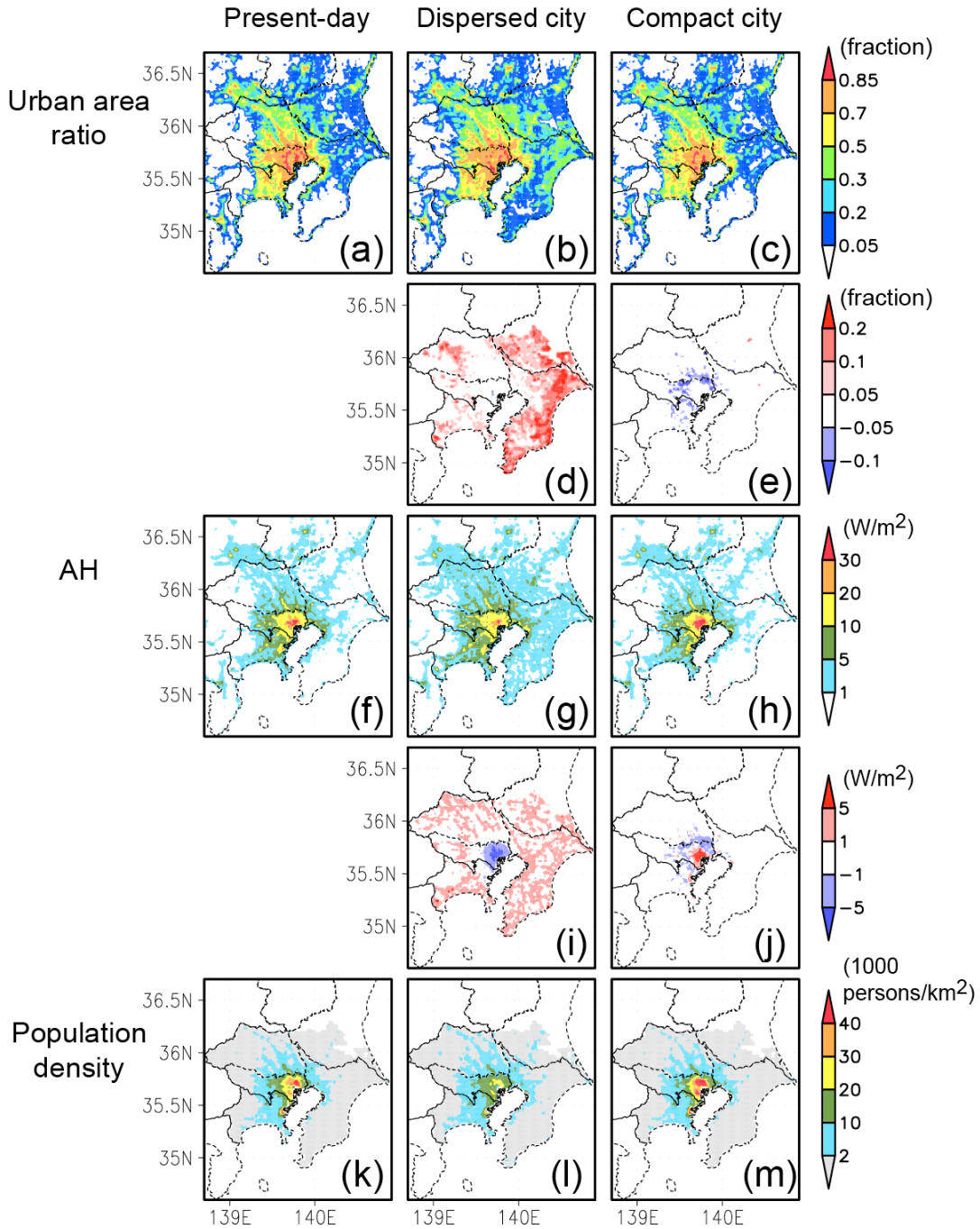

Fig. 2 Distribution of urban parameters: urban area ratio, daily mean anthropogenic heat emission (W m^{-2}), and population per square kilometer in the current urban situation (a, f, and k, respectively), in the dispersed-city scenario (b, g, and l, respectively), and in the compact-city scenario (c, h, and m, respectively). Differences in the urban area ratio and anthropogenic heat flux from the current urban situation are shown in (d) and (i) for the dispersed-city scenario and in (e) and (j) for the compact-city scenario. (Fig.2 in Adachi et al. (2014) ©American Meteorological Society. Used with permission.)

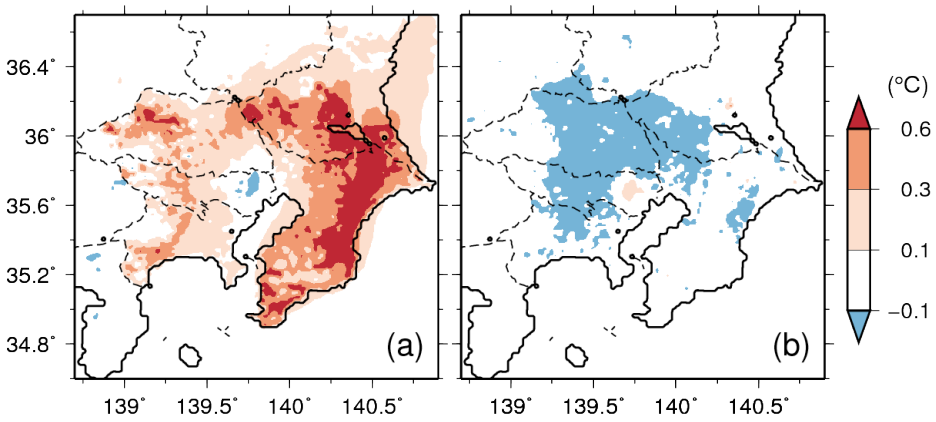

Fig. 3. The differences in monthly nighttime surface air temperature averaged between 01.00 and 05.00 JST in August 2010 for the current urban situation (CTL_o): (a) the dispersed-city scenario (URB_d) and (b) the compact-city scenario (URB_c). (Fig.6 in Adachi et al. (2014) ©American Meteorological Society. Used with permission.)

3. Results

3.1 Nighttime temperature differences due to modification of urban form

The changes in monthly mean nighttime surface air temperature between 01.00 and 05.00 Japan standard time (JST) (hereafter, nighttime temperature) in August due to modification of the urban form are indicated in Fig. 3. A surface air temperature increase was predicted throughout most of the TMA in the dispersed city case (URB_d), with the exception of the central part (Fig. 3a). Warming of more than 0.6°C was simulated in Chiba and Ibaraki prefectures because of the large expansion of urban area in the region (as shown in Fig. 2d). The developed urban area in Tokyo, Kanagawa, and Saitama was projected to experience at most about a 0.3°C temperature increase. However, in the central part of Tokyo, nighttime temperature was projected to decrease by about 0.1°C. In the compact city case, the response of nighttime temperatures to changes in the urban form was opposite to that projected in the dispersed city case. The nighttime temperature was reduced by about 0.1°C over a large area of the TMA, except for the central part, where the temperature increased by about 0.1°C (Fig. 3b). These results indicate that the compact-city scenario had the potential to reduce the intensity of the urban heat island in the whole of the TMA.

3.2 Impact of modification of urban form on thermal comfort

The reduction in nighttime temperature is important in terms of sleep disruption and heatstroke. The compact-city scenario resulted in a reduced nighttime temperature in the TMA, as shown in Figs. 3. However, the nighttime temperature increased in the central part of the TMA, which has a very dense population. Figure 4 shows the population in different areas classified by temperature category, as defined by the monthly mean of daily minimum nighttime temperature (Tminave). The daily minimum nighttime temperature was defined as the minimum temperature between 01.00 JST and 05.00 JST. The population in each temperature category from I to IX was calculated by summing the population in the grid cells that met the conditions of Tminave. In the lower temperature categories (from VI to IX), the population increased in both the URB_d and URB_c simulations. Conversely, the population decreased in the higher temperature categories (II and III) compared with that in the current urban situation. This resulted in a tendency for nighttime temperatures affecting citizens to improve in both urban scenarios. This happened because either people would move into the surrounding areas (Region iii in Fig. 1b) where temperatures were lower in the dispersed-city scenario, or the nighttime temperature would be reduced throughout much of the TMA in the compact-city scenario, as shown in Fig. 6b. However, it should be noted that the population increased by about one million in the highest temperature category (I) in the URB_c simulation. Most people in category I live in the central area of the TMA (i.e., Region i). This resulted in further deterioration in nighttime thermal conditions in the central part of the TMA in the compact-city scenario.

4. Conclusion and Remarks

1) The area-averaged thermal environment during the night tended to deteriorate in the dispersed-city scenario and to improve in the compact-city scenario when compared with the current urban situation.
2) In the central part of the TMA, each urban scenario had the opposite impact on the nighttime surface air temperature, with a temperature increase in the compact-city scenario and a decrease in the

dispersed-city scenario. That is, the severe high temperature conditions worsened in the city center in the compact-city scenario.

3) The results of this study suggest that the compact-city scenario is not always appropriate for the moderation of the urban heat island, especially in the central part of the TMA. To avoid a deterioration of the thermal environment in the central area, the temperature increase needs to be compensated for by other strategies, such as the greening of urban areas.
4) It is important to evaluate an adaptation plan for higher urban temperatures from several perspectives, i.e. not only taking climatological aspects into consideration but also its impacts on urban inhabitants.

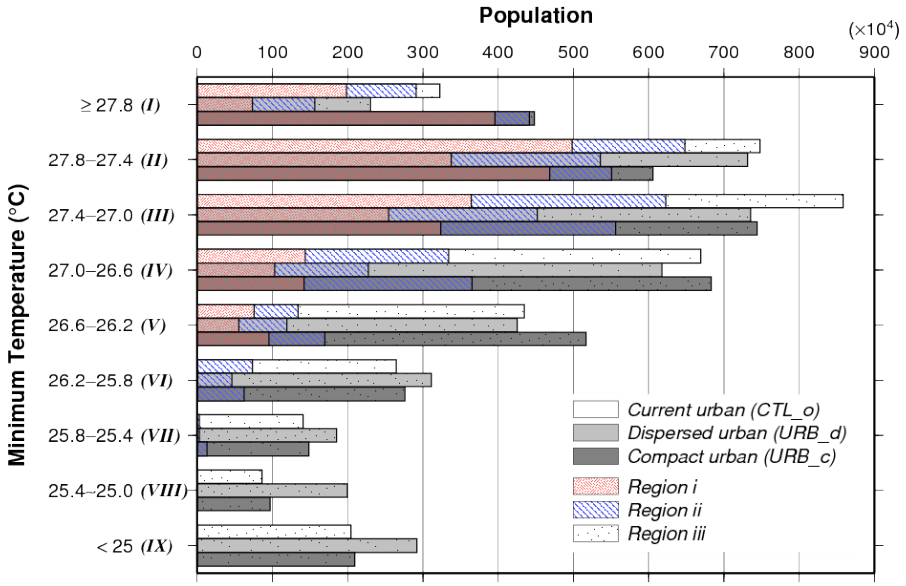

Fig. 4 The relationship between monthly mean daily minimum surface air temperature and the population for a certain grid cell. The daily minimum surface air temperature was defined as the minimum temperature between 01.00 JST and 05.00 JST. Regions i, ii, and iii illustrated indicate where people live, and their locations are defined in Fig. 1b. *(Fig.9 in Adachi et al. (2014) ©American Meteorological Society. Used with permission.)*

Acknowledgment

This study was supported by the GlobalEnvironment Research Fund (S-5-3) of the Ministry of the Environment of Japan and the Research Program on Climate Change Adaptation(RECCA) Fund by Ministry of Education, Culture, Sports, Science and Technology (MEXT) of Japan. First author is supported by the COE project of the Foundation for Computational Science (FOCUS).

References

Adachi, S. A., F. Kimura, H. Kusaka, M. G. Duda, Y. Yamagata, H. Seya, K. Nakamichi, and T. Aoyagi, 2014: Moderation of Summertime Heat Island Phenomena via Modification of the Urban Form in the Tokyo Metropolitan Area. *J. Appl. Meteor. Climatol.,* **53**, 1886–1900. doi: http://dx.doi.org/10.1175/JAMC-D-13-0194.1

Adachi, S. A., F. Kimura, H. Kusaka, T. Inoue, and H. Ueda, 2012: Comparison of the impact of global climate changes and urbanization on summertime future climate in the Tokyo metropolitan area. *J. Appl. Meteor. Climatol.,* **51**(8), 1441–1454, doi:10.1175/JAMC-D-11-0137.1.

Bagan, H., and Y. Yamagata, 2010: Improved subspace classification method for multispectral remote sensing image classification. *Photogrammetric Engineering & Remote Sensing*, **76**(11), 1239–1251.

Kalnay, E., and Coauthors, 1996: The NCEP/NCAR 40-Year Reanalysis Project. *Bull. Amer. Meteor. Soc.*, **77**, 437–471.

Skamarock, W. C., J. B. Klemp, J. Dudhia, D. O. Gill, D. M. Barker, M. G. Duda, X.-Y. Huang, W. Wang, and J. G. Powers, 2008: A Description of the Advanced Research WRF Version 3. *NCAR TECHNICAL NOTE, NCAR/TN-475+STR*.

Yamagata, Y., and H. Seya, 2013: Simulating a future smart city: an integrated land use-energy model. *Appl. Energy*, http://dx.doi.org/10.1016/j.apenergy.2013.01.061.

Yamagata, Y., H. Seya, and K. Nakamichi, 2011: Scenario analysis of the future urban land use in the Tokyo metropolitan area. *Journal of Society of Environmental Science*, **24**(3), 169–179. (in Japanese)

Yamagata, Y., H. Seya, and K. Nakamichi, 2013: Creation of future urban environmental scenarios using a geographically explicit land-use model: a case study of Tokyo, *Annals of GIS*, doi: 10.1080/19475683.2013.806358.